

# Adaptive Feedforward Control with Parameter Estimation for the Chylla–Haase Polymerization Reactor

Knut Graichen, Veit Hagenmeyer, and Michael Zeitz

**Abstract**—An adaptive feedforward control for the Chylla–Haase polymerization reactor is presented in the framework of the two-degree-of-freedom control concept. In order to adapt the feedforward control to different batch conditions and various products, an extended Kalman filter is designed to estimate the reaction heat and the heat transfer coefficient during polymerization. Simulation results under model uncertainties show the effectiveness and accuracy of the adaptive feedforward control concept while maintaining the conventional feedback cascade control.

## I. INTRODUCTION

A control engineering benchmark problem for batch reactors is the polymerization reactor described by Chylla and Haase [2], [3]. The control task comprises the heat-up of the reactor to the operation temperature before the monomer feed starts, and subsequently keeping the temperature constant throughout the polymerization process. Thereby, the step-like profile of the monomer feed poses a significant demand on the control, in order to keep the reactor temperature within a specified tolerance interval. In the benchmark scenario, the operation of the reactor must be guaranteed for two different polymers and under various disturbing influences, e.g. changing ambient temperatures in winter and summer, or impurity of the monomer.

Industrial polymerization reactors are commonly operated with a cascade control structure consisting of a master controller for the reactor temperature and an underlying slave controller for the cooling circuit. The cascade control provides a robust operation, but lacks in control performance. Therefore, various control concepts have been proposed to deal with the benchmark problem. In [6], a model predictive controller is used in combination with an extended Kalman filter. An optimal cooling jacket temperature is calculated in [7] by minimizing a cost function, which keeps the reactor temperature constant in the nominal case. A nonlinear adaptive controller is designed in [4] to adjust the cooling jacket temperature as the setpoint for an underlying PI controller of the cooling jacket. A further contribution [1] deals with the design of a neural network controller to maintain the reactor temperature at its setpoint.

The control concept presented in this contribution solves the Chylla–Haase benchmark problem by extending the conventional cascade feedback control structure with a feedforward control for the cooling jacket temperature. The

feedforward design is based on the inverse energy balance and calculates a feedforward trajectory for the cooling jacket temperature in order to follow a predefined desired trajectory of the reactor temperature. Thereby, the reaction heat as well as the heat transfer coefficient in the energy balance are estimated online by an extended Kalman filter.

The paper is organized as follows: Section II describes the Chylla–Haase control problem and the reactor model. The conventional cascade control structure is explained as the basis for the proposed control scheme. In Section III, an extended Kalman filter is designed to estimate the states as well as the reaction heat and the heat transfer coefficient. These estimates are used for the adapted calculation of the inversion-based feedforward control in Section IV. Simulation results are given in Section V for various batch scenarios and model mismatches to illustrate the accuracy and robustness of the proposed control scheme.

## II. THE CHYLLA–HAASE REACTOR BENCHMARK

The industrial polymerization reactor described by Chylla and Haase [2], [3] consists of a stirred tank reactor with a cooling jacket and a coolant recirculation, see Fig. 1. The reactor temperature is influenced by manipulating the temperature of the coolant which is recirculated through the cooling jacket of the reactor. The slave controller can act in two modes: in cooling mode, cold water is inserted into the recirculation loop, whereas in heating mode steam is injected into the circulating water stream. In [2], the production of two different polymers  $A$  and  $B$  is considered. The respective recipes comprise the following control tasks:

- heating up of the reactor to a constant setpoint before the monomer feed  $\dot{m}_M^{in}(t)$  starts,
- keeping the reactor temperature at its setpoint within a tolerance interval of  $\pm 0.6$  K during the monomer feed and after a subsequent specified hold period.

Thereby, the monomer feed  $\dot{m}_M^{in}(t)$  starts and ends abruptly at specified time points. The respective polymer  $A$  or  $B$  is produced in five subsequent batches, and is removed between the batches. However, the reactor is only cleaned after the fifth batch. The control tasks are complicated by the following features and constraints of the reactor [2]:

- The production of polymers  $A$  and  $B$  is subject to different reaction kinetics and reaction heats.
- The heat transfer coefficient decreases significantly during a batch due to an increasing batch viscosity, and from batch to batch due to surface fouling.
- The reaction kinetics are nonlinear and subject to the gel effect.

K. Graichen and M. Zeitz are with Institut für Systemdynamik und Regelungstechnik, Universität Stuttgart, D-70550 Stuttgart, Germany {graichen, zeitz}@isr.uni-stuttgart.de

V. Hagenmeyer is with BASF Aktiengesellschaft, Ludwigshafen, Germany veit.hagenmeyer@basf-ag.de

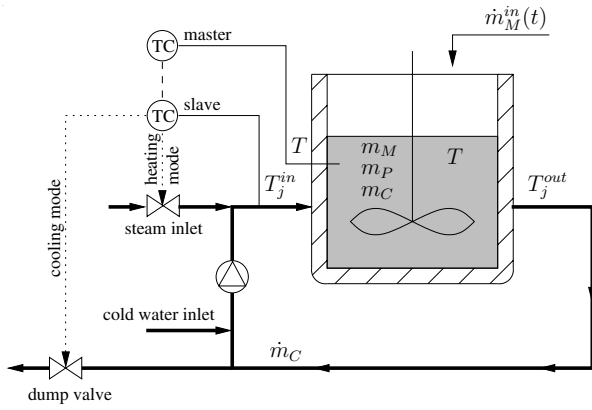


Fig. 1. Reactor schematic with cooling recirculation loop, monomer feed  $\dot{m}_M^{in}(t)$ , master and slave controller (TC = temperature controller).

### A. Polymerization reactor model

A dynamic model of the polymerization reactor has been derived by Chylla and Haase [2] based on simplified kinetic relations, also see the corrigenda [3]. The temperature dynamics are described by energy balances for the reactor and the cooling jacket. However, some corrections must be considered:

- A corrected energy balance for the reactor temperature is derived in [6].
- The precharge of the reactor consisting of prepolymer  $m_{P,0}$  and water  $m_W$  as given in the original paper [2] exceeds the reactor volume, see [6]. This problem is addressed in [7] by assuming smaller values such that the reactor volume is not exceeded after polymerization.
- The heat transfer coefficient between wall and reactor falls to zero during the production of polymer  $B$ , making it impossible to further control the reactor temperature. Therefore, the heat transfer coefficient is limited to a minimum value of  $0.2 \text{ kW m}^{-2} \text{ K}^{-1}$  [6].

The corrected reference model of the Chylla–Haase reactor is given by

$$\frac{dm_M}{dt} = \dot{m}_M^{in}(t) + \frac{Q_{rea}}{\Delta H} \quad (1)$$

$$\frac{dm_P}{dt} = -\frac{Q_{rea}}{\Delta H} \quad (2)$$

$$\frac{dT}{dt} = \frac{1}{\sum_i m_i C_{p,i}} \left[ \dot{m}_M^{in}(t) C_{p,M} (T_{amb} - T) + Q_{rea} - UA(T - T_j) - (UA)_{loss}(T - T_{amb}) \right], \quad i = M, P, W \quad (3)$$

$$\frac{dT_j^{out}}{dt} = \frac{1}{m_C C_{p,C}} \left[ \dot{m}_C C_{p,C} (T_j^{in}(t - \theta_1) - T_j^{out}) + UA(T - T_j) \right] \quad (4)$$

$$\frac{dT_j^{in}}{dt} = \frac{dT_j^{out}(t - \theta_2)}{dt} + \frac{T_j^{out}(t - \theta_2) - T_j^{in}}{\tau_p} + \frac{K_p(c)}{\tau_p} \quad (5)$$

The reactor model comprises the material balances (1)–(2) for the monomer  $M$  and the polymer  $P$ , the energy balance (3) for the reactor temperature  $T(t)$ , as well as the energy

balances (4)–(5) of the cooling jacket and the recirculation loop with the inlet and outlet temperatures  $T_j^{out}(t)$  and  $T_j^{in}(t)$  of the coolant  $C$ .

The polymerization rate  $R_p = Q_{rea}/(-\Delta H)$ , the jacket heat transfer area  $A$  and the heat transfer coefficient  $U$  are modeled with empirical relations taken from [2], [7]. Due to the lack of space, these relations and the data of the model parameters are omitted here and only their functional dependency on the states is given in Table I.

The heating/cooling function  $K_p(c)$ , as defined in [2], [3], is influenced by an equal–percentage valve with position  $c(t)$  and the following split–range valve characteristic

$$K_p(c) = \begin{cases} 0.8 \cdot 30^{-c/50} (T_{inlet} - T_j^{in}) & c < 50\% \\ 0 & c = 50\% \\ 0.15 \cdot 30^{(c/50-2)} (T_{steam} - T_j^{in}) & c > 50\% \end{cases}$$

For  $c < 50\%$ , ice water with inlet temperature  $T_{inlet}$  is inserted in the cooling jacket, whereas a valve position  $c > 50\%$  leads to a heating of the coolant by injecting steam with temperature  $T_{steam}$  into the circulating water stream.

The time intervals of the monomer feed  $\dot{m}_M^{in}(t)$  are specified in the recipes for polymer  $A$  and  $B$  [2]. For polymer  $A$ , a single feed interval  $t \in [30 \text{ min}, 100 \text{ min}]$  is considered, whereas the recipe of polymer  $B$  comprises two feed periods  $t \in [30 \text{ min}, 90 \text{ min}]$  and  $t \in [120 \text{ min}, 160 \text{ min}]$  with a specified hold period between the two feeds. The first time interval before the monomer feed starts accounts for the heat–up of the reactor with the heat–up time  $t_{heat} = 30 \text{ min}$ .

### B. Conventional cascade feedback control structure

A very tight temperature control is necessary in order to produce polymer of a desired quality. The controller should be able to keep the reactor temperature  $T$  within an interval of  $\pm 0.6 \text{ K}$  around the desired setpoint under all operating conditions and disturbances [2]. Commonly used for chemical reactors is a PI cascade control structure, which provides a robust operation but often lacks in control performance. The cascade control structure is shown in Fig. 2 as the basis for the adaptive feedforward control concept proposed in this paper. The master controller  $\Sigma_{FB,1}$  regulates the reactor

TABLE I  
PARAMETERS OF THE REACTOR MODEL (1)–(5) (DATA IN [2], [7]).

$\dot{m}_M^{in}(t)$	monomer feed rate [kg/s]
$Q_{rea} = R_p(-\Delta H)$	reaction heat [kW]
$R_p(m_M, m_P, T)$	rate of polymerization [kg/s]
$-\Delta H$	reaction enthalpy [kJ/kg]
$U(T, T_j)$	overall heat transfer coeff. [kW/(m <sup>2</sup> K)]
$A(m_M, m_P)$	jacket heat transfer area [m <sup>2</sup> ]
$(UA)_{loss}$	heat loss coefficient [kW/K]
$C_{p,M}, C_{p,P}, C_{p,C}$	specific heat at const. pressure [kJ/(kg K)]
$\theta_1, \theta_2$	transport delay in jacket and recirc. loop [s]
$T_j = (T_j^{in} - T_j^{out})/2$	mean jacket temperature [K]
$\tau_p$	heating/cooling time constant [s]
$K_p(c)$	heating/cooling function [K]
$c$	valve position [%]
$T_{inlet}$	water inlet temperature [K]
$T_{steam}$	steam temperature [K]

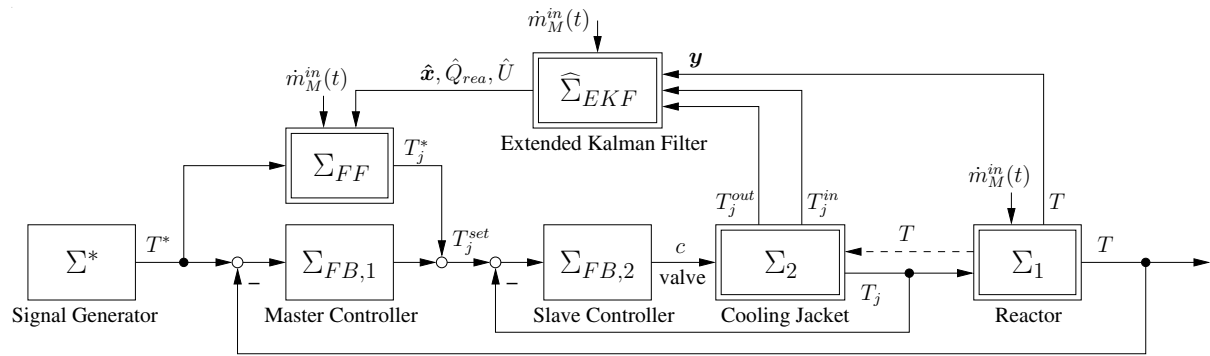


Fig. 2. Adaptive control scheme with reactor model  $\Sigma_1$  : (1)–(3), cooling circuit model  $\Sigma_2$  : (4)–(5), master and slave controller  $\Sigma_{FB,1}$  and  $\Sigma_{FB,2}$ , adaptive feedforward control  $\Sigma_{FF}$ , and extended Kalman filter  $\widehat{\Sigma}_{EKF}$ .

temperature  $T$  by manipulating the setpoint  $T_j^{set}$  of the mean cooling jacket temperature  $T_j$ . The slave controller  $\Sigma_{FB,2}$  adjusts the valve position  $c$  in order to control the mean jacket temperature  $T_j$  set by the master controller.<sup>1</sup>

In order to heat-up the reactor before the monomer feed starts, a sufficiently smooth polynomial trajectory  $T^*(t)$  for the reactor temperature is generated with the boundary conditions  $T^*(0) = T_{amb}$  and  $T^*(t_{heat}) = T_{set}$  as setpoint for the polymerization. After the heat-up interval,  $T^*(t)$  remains constant.

The simulation results of the reactor with the PI cascade control for polymer A and B are shown in Fig. 3 for the batches 1 and 5.<sup>2</sup> The sampling times for the slave and the master controller are set to 4 s. A tracking error  $\Delta T$  occurs during the heat-up interval, since the reactor temperature  $T(t)$  follows the desired trajectory  $T^*(t)$  only time-delayed. During the polymerization, the reactor temperature  $T(t)$  violates the tolerance interval  $\pm 0.6$  K especially at the end of the monomer feed. The temperature error  $\Delta T$  is larger during batch no. 5, since the heat transfer coefficient  $U$  decreases significantly during the successive batches, see Fig. 4.

### C. Adaptive control concept

The performance of the cascade control can be significantly improved by an additional feedforward control in the framework of the two-degree-of-freedom control structure, see Fig. 2. The feedforward control  $\Sigma_{FF}$  injects the feedforward trajectory  $T_j^*(t)$  such that the overall setpoint for the mean jacket temperature becomes

$$T_j^{set} = T_j^* + \Delta T_{j,FB,1}. \quad (6)$$

The feedback part  $\Delta T_{j,FB,1}$  of the master controller  $\Sigma_{FB,1}$  stabilizes the reactor temperature along the desired trajectory  $T^*(t)$ .

A process control which universally allows the production of multiple polymers requires to calculate the feedforward

<sup>1</sup>Commonly, the jacket inlet temperature  $T_j^{in}$  is used as the manipulating variable for the control of the reactor temperature. Here,  $T_j = (T_j^{in} + T_j^{out})/2$  (see Table I) is used instead of  $T_j^{in}$ , because  $T_j$  appears explicitly in the energy balance (3) of the reactor model.

<sup>2</sup>The parameters of the cascade control have been tuned in simulation studies to  $K_P^m = 4$ ,  $T_I^m = 20$  s for the master controller, and to  $K_P^s = 20$ ,  $T_I^s = 40$  s for the slave controller. These values are also used as controller parameters in the following sections.

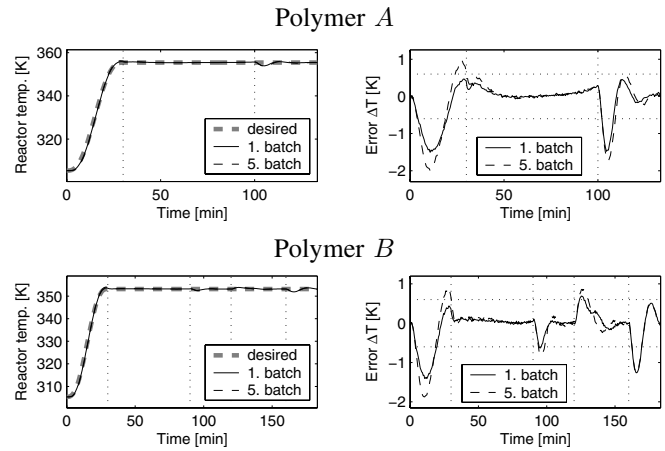


Fig. 3. Reactor temperature  $T(t)$  and control error  $\Delta T(t)$  of the PI cascade controlled reactor for polymer A and B, nominal parameters and summer season.

control adaptively based on an online estimation of the reaction heat  $Q_{rea}(t)$  and heat transfer coefficient  $U(t)$  during the successive batches. Therefore, an extended Kalman filter (EKF)  $\widehat{\Sigma}_{EKF}$  is designed which uses the available temperature measurements to estimate  $\widehat{Q}_{rea}(t)$  and  $\widehat{U}(t)$ , see Fig. 2. These estimates are used for the adaption of the feedforward control  $\Sigma_{FF}$ , as explained in the following sections.

## III. PARAMETER ESTIMATION WITH EXTENDED KALMAN FILTER

An online estimation of the time-dependent reaction heat  $Q_{rea}(t)$  and overall heat transfer coefficient  $U(t)$  with an EKF requires a simplified reactor model, which is still accurate enough to obtain reliable estimates. The reference model is reduced by omitting the energy balance (5) for the recirculation loop. This is motivated by the fact that the reaction heat  $Q_{rea}(t)$  and the overall heat transfer coefficient  $U(t)$  only occur in the energy balances (3) and (4) of the reactor and the cooling jacket. To compensate for the omission of the ODE (5), the instantaneous and the time-delayed measurements of the inlet temperature  $T_j^{in}$  are used in the EKF as known variables

$$\eta_1(t) = T_j^{in}(t), \quad \eta_2(t) = T_j^{in}(t - \theta_1), \quad (7)$$

which yields the simplified reactor model

$$\frac{dm_M}{dt} = \dot{m}_M^{in}(t) + \frac{Q_{rea}}{\Delta H} \quad (8)$$

$$\frac{dm_P}{dt} = -\frac{Q_{rea}}{\Delta H} \quad (9)$$

$$\frac{dT}{dt} = \frac{1}{\sum_i m_i C_{p,i}} \left[ \dot{m}_M^{in}(t) C_{p,M} (T_{amb} - T) + Q_{rea} - UA(T - T_j(\eta_1)) - (UA)_{loss}(T - T_{amb}) \right], \quad (10)$$

$$\frac{dT_j^{out}}{dt} = \frac{1}{m_C C_{p,C}} \left[ \dot{m}_C C_{p,C} (\eta_2 - T_j^{out}) + UA(T - T_j(\eta_1)) \right] \quad (11)$$

with the mean jacket temperature

$$T_j(\eta_1) = \frac{T_j^{out} - \eta_1}{2}. \quad (12)$$

This simplified model is used for the design of the EKF with the measurement vector  $\mathbf{y} = [T, T_j^{out}]^T$ .<sup>3</sup>

Furthermore, model equations are required for the simultaneous estimation of  $Q_{rea}(t)$  and  $U(t)$ , which is a challenging problem due to the highly nonlinear dynamics of the reactor. The gray profiles (- -) in Fig. 4 show nominal values of  $Q_{rea}(t)$  and  $U(t)$  for polymer *A* calculated with the reference reactor model (1)–(5). The reaction heat  $Q_{rea}(t)$  shows sharp flanks at the beginning and especially at the end of the reaction when the monomer feed  $\dot{m}_M^{in}(t)$  stops. Furthermore, the heat transfer coefficient  $U(t)$  decreases significantly during the polymerization and successive batches as viscosity at the wall increases.

In order to be universally applicable to multiple polymers, an attempt is made to model the reaction heat  $Q_{rea}(t)$  and the heat transfer coefficient  $U(t)$  without using detailed process knowledge. The reaction heat is modeled by physically reasoning that

$$Q_{rea}(t) = q_0 m_M(t), \quad (13)$$

which relates  $Q_{rea}(t)$  to the monomer mass  $m_M(t)$  in dependence of a factor  $q_0$ , which has to be estimated instead of directly estimating  $Q_{rea}(t)$ . The relation (13) couples the reaction heat  $Q_{rea}(t)$  to the monomer feed  $\dot{m}_M^{in}(t)$  via the material balance (8). This has the advantage that the sharp fall of the reaction heat at the time instant when the monomer feed stops can be detected without any time delay.

In a similar manner, the heat transfer coefficient  $U(t)$  is modeled by reasoning that  $U(t)$  decreases during the process due to the increase of viscosity at the reactor wall, which again is related to the increasing polymer mass  $m_P(t)$ . Therefore, the relation

$$U(t) = U_0 + q_1(m_P(t) - m_{P,0}) \quad (14)$$

is assumed, where  $U_0$  is the heat transfer coefficient before the polymerization starts. The second term in (14) accounts for the decrease of  $U(t)$  during the polymerization with the

simultaneous increase of produced polymer ( $m_P(t) - m_{P,0}$ ), whereby  $m_{P,0}$  is the precharge of the reactor. In view of (13) and (14), the EKF is augmented by three ODEs

$$\dot{q}_0 = 0, \quad \dot{U}_0 = 0, \quad \dot{q}_1 = 0, \quad (15)$$

for the parameters  $q_0$ ,  $U_0$ , and  $q_1$ . This yields the overall estimation vector  $\hat{\mathbf{x}} = [\hat{m}_M, \hat{m}_P, \hat{T}, \hat{T}_j^{out}, \hat{q}_0, \hat{U}_0, \hat{q}_1]^T$  with the respective initial condition

$$\hat{\mathbf{x}}(0) = [m_{M,0}, m_{P,0}, T_{amb}, T_{amb}, \hat{q}_0(0), \hat{U}_0(0), 0]^T. \quad (16)$$

The initial values  $\hat{q}_0(0)$  and  $\hat{U}_0(0)$  are determined by the respective values of the previous batch when the monomer feed starts.

The uncertainties of the system are modeled as process noise in the covariance matrix of the EKF with the diagonal elements listed in Table II. The case-dependent choice of  $\sigma^2(\hat{U}_0)$  and  $\sigma^2(\hat{q}_1)$  is used to estimate  $\hat{U}_0(t)$  during the heat-up before the polymerization starts, and afterwards to estimate  $\hat{q}_1(t)$ , respectively. Process noise is added to the energy balance (11) of the cooling jacket to account for the uncertainties in the delay time  $\theta_1$  [2]. Furthermore, the values of  $\sigma^2(\hat{q}_1)$  and  $\sigma^2(\hat{T}_j^{out})$  are smaller during the monomer feed interval in order to accurately estimate the significant decrease of the heat transfer coefficient  $\hat{U}(t)$  via  $\hat{q}_1(t)$  in (14).<sup>4</sup> The covariance matrix of the measurement noise is set to  $\text{diag}(\sigma^2(y_1), \sigma^2(y_2))$ , whereby noise is added to the measurements  $\mathbf{y} = [T, T_j^{out}]^T$  with the standard deviation  $\sigma(y_1) = \sigma(y_2) = 0.02$  K. The sampling time of the EKF is set to  $\Delta t_{EKF} = 4$  s.

Fig. 4 shows the estimated profiles of  $\hat{m}_M(t)$ ,  $\hat{m}_P(t)$ ,  $\hat{Q}_{rea}(t)$ , and  $\hat{U}(t)$  for polymer *A* compared to the nominal values (- -). The EKF achieves good estimates of  $Q_{rea}(t)$  and  $U(t)$ . Especially the sharp flanks of the reaction heat  $Q_{rea}(t)$  at the beginning and the end of the monomer feed are detected without any time delay, which is essential in order to use the EKF for the adaptive feedforward control design.

TABLE II

DIAGONAL ENTRIES IN THE PROCESS NOISE COVARIANCE MATRIX.

Entries in $Q$	Unit	heat-up period	1. feed period	hold period
$\sigma^2(\hat{m}_M)$	[kg]	0	0	0
$\sigma^2(\hat{m}_P)$	[kg]	0	0	0
$\sigma^2(\hat{T})$	[K <sup>2</sup> ]	0	0	0
$\sigma^2(\hat{T}_j^{out})$	[K <sup>2</sup> ]	$5 \cdot 10^{-3}$	$5 \cdot 10^{-4}$	$5 \cdot 10^{-3}$
$\sigma^2(\hat{q}_0)$	$[\frac{\text{kW}^2}{\text{kg}^2}]$	$5 \cdot 10^{-3}$	$5 \cdot 10^{-3}$	$5 \cdot 10^{-3}$
$\sigma^2(\hat{U}_0)$	$[\frac{\text{kW}^2}{\text{m}^4 \text{K}^2}]$	$5 \cdot 10^{-8}$	0	0
$\sigma^2(\hat{q}_1)$	$[\frac{\text{kW}^2}{\text{m}^4 \text{K}^2 \text{kg}^2}]$	0	$5 \cdot 10^{-8}$	$5 \cdot 10^{-9}$

<sup>3</sup>Note that the measurement of  $T_j^{in}$  is used for the definition (7) of the variables  $\eta_1(t)$  and  $\eta_2(t)$  in (8)–(12).

<sup>4</sup>For the second feed period of polymer *B*, the parameter settings remain constant after the first hold period, see Table II.

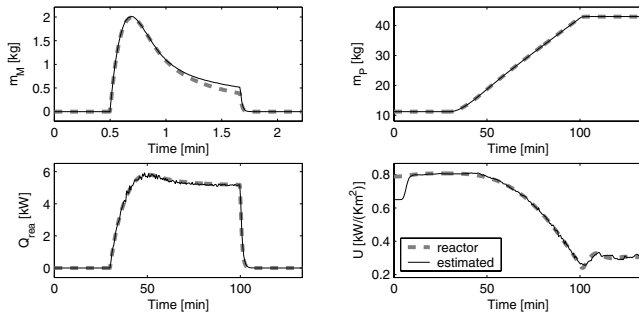


Fig. 4. Simulation results for polymer A: Kalman estimates of the reactor with PI cascade control for batch 1, nominal parameters, and summer season.

#### IV. ADAPTIVE FEEDFORWARD CONTROL DESIGN

The inversion-based feedforward control design [5] is based on the input–output normal form of the reactor model (1)–(3). Thereby, the energy balance (3) for the output  $T$  forms the input–output dynamics, whereas the material balances (1)–(2) represent the internal dynamics. The inverse of the input–output dynamics (3) allows the calculation of the feedforward control

$$T_j^* = T^* + \frac{1}{U^* A} \left[ \dot{T}^* \sum_{i=M,P,W} m_i^* C_{p,i} - Q_{rea}^* - \dot{m}_M^{in}(t) C_{p,M} (T_{amb} - T^*) + (UA)_{loss} (T^* - T_{amb}) \right] \quad (17)$$

in dependence of the desired reactor temperature  $T^*(t) \in \mathcal{C}^1$  and the trajectories  $m_M^*(t)$ ,  $m_P^*(t)$ ,  $Q_{rea}^*(t)$ ,  $U^*(t)$ , which have to be determined for the calculation of (17). Note that the monomer feed rate  $\dot{m}_M^{in}(t)$  appears as time-varying parameter in (17).

The adaptive design calculates the feedforward control (17) in each time instant  $t_k$  over the next time interval  $t \in [t_k, t_{k+1}]$ . Thereby, the interval length  $\Delta t_{FF} = t_{k+1} - t_k$  is given by the feedforward sampling time. The trajectories  $m_M^*(t)$  and  $m_P^*(t)$  of the monomer and polymer are calculated by integrating the internal dynamics, i.e. the material balances (1)–(2) with (13), over the time interval  $t \in [t_k, t_{k+1}]$ :

$$\dot{m}_M^* = \dot{m}_M^{in}(t) + \frac{\hat{q}_0(t_k) m_M^*(t)}{\Delta H}, \quad (18)$$

$$\dot{m}_P^* = -\frac{\hat{q}_0(t_k) m_M^*(t)}{\Delta H}. \quad (19)$$

The initial values  $m_M(t_k) = \hat{m}_M(t_k)$ ,  $m_P(t_k) = \hat{m}_P(t_k)$  as well as  $\hat{q}_0(t_k)$  are provided by the EKF at time instant  $t_k$ .

With the trajectories  $m_M^*(t)$  and  $m_P^*(t)$ , the reaction heat and the heat transfer coefficient are given by

$$Q_{rea}^*(t) = \hat{q}_0(t_k) m_M^*(t), \quad (20)$$

$$U^*(t) = \hat{U}_0(t_k) + \hat{q}_1(t_k) (m_P^*(t) - m_{P,0}) \quad (21)$$

for  $t \in [t_k, t_{k+1}]$ . Placing  $m_M^*(t)$ ,  $m_P^*(t)$ , and (20)–(21) in (17) finally yields the feedforward control  $T_j^*(t)$  for the time interval  $t \in [t_k, t_{k+1}]$ , which is used for the setpoint (6) of the slave controller.

#### V. SIMULATION RESULTS

The simulation results for both polymers A and B, and nominal parameter values are depicted in the Figs. 5 and 6. To illustrate the robustness of the online control scheme, a mismatch of +25% is considered in both delay times  $\theta_1$  and  $\theta_2$ , as well as an increased rate of polymerization by +20% which accounts for impurity of the monomer [2], see Figs. 7 and 8. The feedforward control clearly improves the control performance and the control error  $\Delta T(t)$  stays within the tolerance interval of  $\pm 0.6$  K. Especially at the critical time points when the monomer feed stops, the feedforward control  $T_j^*(t)$  sharply increases to compensate for the step-like decrease of the reaction heat  $Q_{rea}(t)$ . This is mainly due to EKF relations (13) and (20), which enable the fast detection of the sharp flank of the reaction heat  $Q_{rea}(t)$  at the end of the monomer feed. Furthermore, the mismatch scenario in the Figs. 7 and 8 shows the robustness of the EKF and the adaptive feedforward control, particularly in combination with the conventional PI cascade control.

#### VI. CONCLUSIONS

The extension of a conventional cascade control by a feedforward part is proposed for the polymerization reactor benchmark problem defined by Chylla and Haase. The feedforward control clearly improves the control performance while maintaining the standard cascade feedback control structure, which is of importance for industrial applications. The resulting two-degree-of-freedom control scheme uses an extended Kalman filter for the online adaptation of the feedforward control. The fast detection of the falling flank at the end of the reaction is crucial for the performance of the feedforward control. Therefore, physically motivated relations for the heat transfer coefficient and the reaction heat are derived, which provide an accurate estimate. Especially the reaction heat is estimated without any time delay. These relations are not based on exact process knowledge and are therefore applicable to a wider range of batch reactors.

#### REFERENCES

- [1] A. Bhat and R.N. Banavar, The Chylla-Haase-Problem: A neural network controller, in *Proc. IEEE Int. Conf. Contr. Appl.*, Trieste/Italy, 1998, pp. 192–196.
- [2] R.W. Chylla and D.R. Haase, Temperature control of semi-batch polymerization reactors, *Comput. Chem. Eng.*, vol. 17, 1993, pp. 257–264.
- [3] R.W. Chylla and D.R. Haase, Temperature control of semi-batch polymerization reactors (corrigenda), *Comput. Chem. Eng.*, vol. 17, 1993, p. 1213.
- [4] T. Clarke-Pringle and J.F. MacGregor, Nonlinear adaptive temperature control of multi-product, semi-batch polymerization reactors, *Computers chem. Engng.*, vol. 21, 1997, pp. 1395–1409.
- [5] S. Devasia, D. Chen, and B. Paden, Nonlinear inversion-based output tracking, *IEEE Trans. Automat. Contr.*, vol. 41, 1996, pp. 930–942.
- [6] A. Helbig, O. Abel, A. M'hamdi, and W. Marquardt, Analysis and nonlinear model predictive control of the Chylla-Haase benchmark problem, in *Proc. UKACC Int. Conf. Control*, Exeter/England, 1996, pp. 1172–1177.
- [7] H. Hinsberger, S. Miesbach, and H.J. Pesch, Optimal temperature control of semibatch polymerization reactors, in F. Keil, W. Mackens, H. Voß, and J. Werther (editors): *Scientific Computing in Chemical Engineering*, Springer, 1996, pp. 75–83.

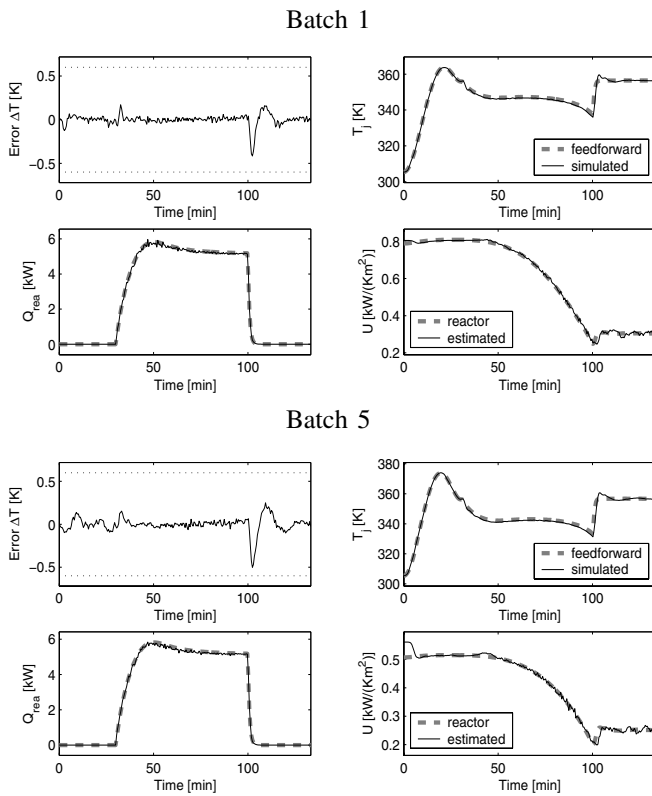


Fig. 5. Simulation results for polymer A, batch no. 1 and 5: Adaptive feedforward control with PI cascade control for nominal parameters, and summer season.

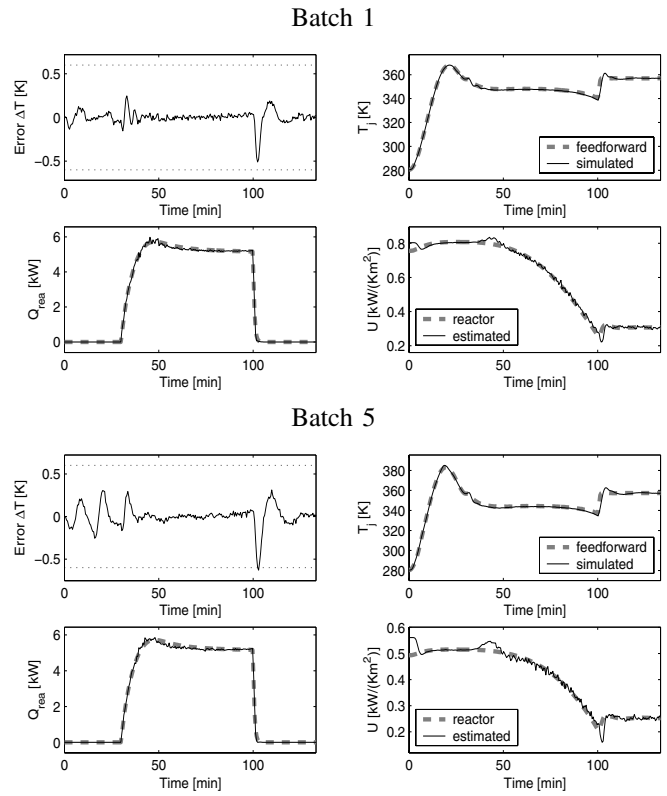


Fig. 7. Simulation results for polymer A, batch no. 1 and 5: Adaptive feedforward control with PI cascade control for delay times  $\theta_1, \theta_2 \pm 25\%$ , +20% higher rate of polymerization, and winter season.

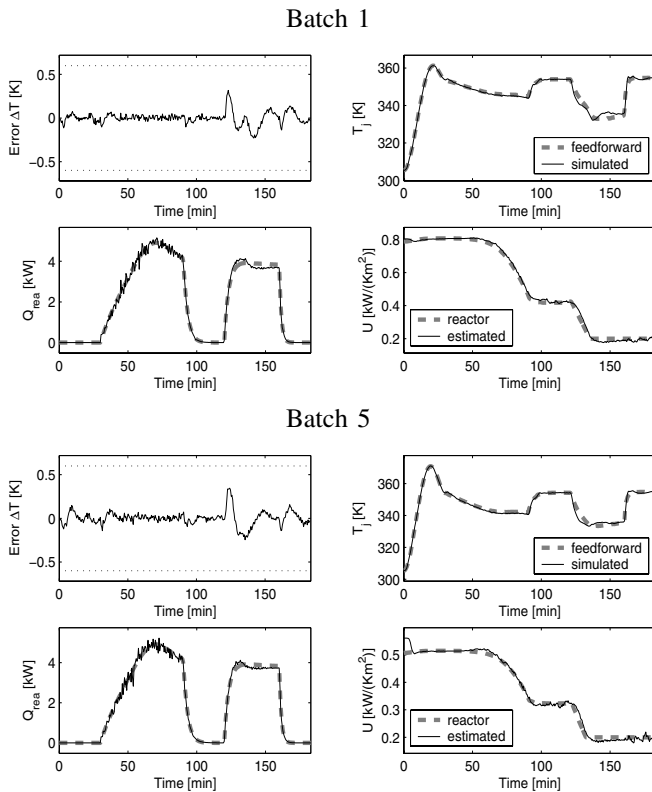


Fig. 6. Simulation results for polymer B, batch no. 1 and 5: Adaptive feedforward control with PI cascade control for nominal parameters, and summer season.

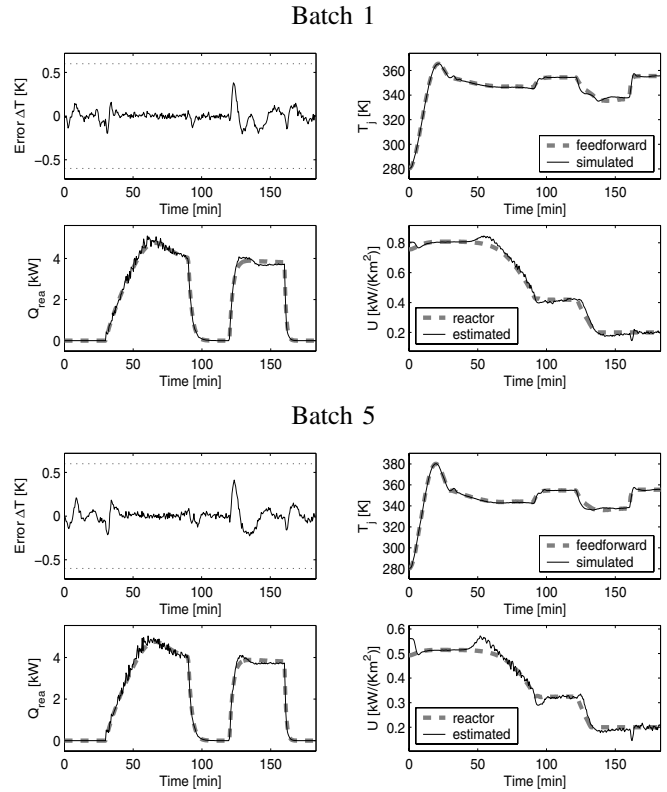


Fig. 8. Simulation results for polymer B, batch no. 1 and 5: Adaptive feedforward control with PI cascade control for delay times  $\theta_1, \theta_2 \pm 25\%$ , +20% higher rate of polymerization, and winter season.